

# Analysis of Electrical Characteristics of Edge-Coupled Microstrip Lines with a Dielectric Overlay

BARRY E. SPIELMAN

*Microwave Techniques Branch  
Electronics Division*

October 25, 1974



**NAVAL RESEARCH LABORATORY**  
**Washington, D.C.**



SECURITY CLASSIFICATION OF THIS PAGE (When Data Entered)

REPORT DOCUMENTATION PAGE		READ INSTRUCTIONS BEFORE COMPLETING FORM
1. REPORT NUMBER NRL Report 7810	2. GOVT ACCESSION NO.	3. RECIPIENT'S CATALOG NUMBER
4. TITLE (and Subtitle)  ANALYSIS OF ELECTRICAL CHARACTERISTICS OF EDGE-COUPLED MICROSTRIP LINES WITH A DIELEC- TRIC OVERLAY		5. TYPE OF REPORT & PERIOD COVERED Interim report on continuing NRL Problems
		6. PERFORMING ORG. REPORT NUMBER
7. AUTHOR(s) Barry E. Spielman		8. CONTRACT OR GRANT NUMBER(s) NRL Problems R08-36 and R08-63; XF 54-545-007 and RR 021-03-46-5630
9. PERFORMING ORGANIZATION NAME AND ADDRESS Naval Research Laboratory Washington, D.C. 20375		10. PROGRAM ELEMENT, PROJECT, TASK AREA & WORK UNIT NUMBERS
11. CONTROLLING OFFICE NAME AND ADDRESS Department of the Navy    Naval Electronics Systems Office of Naval Research    Command, Arlington, Va. 22217    Washington, D.C. 20360		12. REPORT DATE October 25, 1974
		13. NUMBER OF PAGES 40
14. MONITORING AGENCY NAME & ADDRESS (if different from Controlling Office)		15. SECURITY CLASS. (of this report) Unclassified
		15a. DECLASSIFICATION/DOWNGRADING SCHEDULE
16. DISTRIBUTION STATEMENT (of this Report)  Approved for public release; distribution unlimited.		
17. DISTRIBUTION STATEMENT (of the abstract entered in Block 20, if different from Report)		
18. SUPPLEMENTARY NOTES		
19. KEY WORDS (Continue on reverse side if necessary and identify by block number)  Broadband microstrip components      Directional filters Computer-aided analysis      Microwave integrated circuits Coupled strip transmission lines      Schiffman phase shifters Directional couplers		
20. ABSTRACT (Continue on reverse side if necessary and identify by block number) An analysis has been performed of the electrical characteristics of edge-coupled microstrip lines with a dielectric overlay. This analysis is applicable to the design of broadband directional couplers, filters, and Schiffman phase shifters for microwave integrated circuit applications. The analysis incorporated an even- and odd-mode treatment that invokes a quasi-TEM propagation model. This treatment enabled the analysis to be formulated in terms of integro-differential equations involving equivalent sources at conductor and dielectric boundaries. The formulation was reduced to a form  (Continued)		

## 20. ABSTRACT

suitable for numerical solution by employing a method-of-moment solution with pulse expansions of equivalent sources and point matching of the boundary conditions.

The analysis was implemented by a digital computer program that provides information on midband coupling, modal impedances, coupled line characteristic impedance, modal phase velocities, and coupled line phase velocities. The program generated design curves that can be used in the design of directional couplers, filters, and Schiffman phase shifters. A comparison of calculated and measured characteristics for three different experimental, two-section, directional couplers demonstrated the accuracy of the computer-aided analysis.

## CONTENTS

INTRODUCTION .....	1
Background .....	1
Format.....	2
ANALYSIS .....	2
Integro-Differential Formulation .....	2
Method-of-Moments Reduction .....	5
Determination of Even- and Odd-Mode Transmission-Line Parameters .....	8
COMPUTER PROGRAM.....	10
General Considerations .....	11
Input Information .....	11
Output Information.....	12
Experimental Verification of Program MICDOC .....	13
DESIGN CURVES.....	19
DISCUSSION.....	22
ACKNOWLEDGMENT .....	23
REFERENCES .....	24
APPENDIX A — Listing of Program MICDOC .....	25



## ANALYSIS OF ELECTRICAL CHARACTERISTICS OF EDGE-COUPLED MICROSTRIP LINES WITH A DIELECTRIC OVERLAY

### INTRODUCTION

#### Background

Considerable interest exists in developing broadband electronic systems using microwave integrated circuits (MICs). Such systems can have the following advantages:

1. Reasonable performance
2. Savings in fabrication costs when production quantities are sufficient to reap the advantages of photolithographic and thin-film techniques
3. Savings in size and weight because of the availability of ceramics of high dielectric constant
4. Reliability
5. The ease with which lumped element control devices and circuit elements can be incorporated.

Many of the circuit functions necessary for MIC systems can be realized using microstrip as the primary transmission line. These realizations draw heavily from the abundance of design and development information on shielded strip line components and systems.

Some difficulties have been encountered in the application of shielded strip line design techniques to the development of high-performance, broadband, microstrip, directional couplers and hybrids. A common approach for implementing such components in shielded strip line is to appropriately interconnect quarter-wavelength long (at midband) sections of parallel, coupled lines. One problem in implementing such components in microstrip is that, for loosely coupled sections of edge-coupled microstrip, the inhomogeneity of the dielectric media limits the isolation characteristic. It has been shown [1] that this effect is attributable to a difference between the even- and odd-mode phase velocities. Another problem is the difficulty in achieving sufficiently strong coupling in a single section of parallel coupled lines by a microstrip approach compatible with current limitations of photolithographic and thin-film fabrication tolerances.

A coupled line configuration that is compatible with an MIC format and offers some relief for the directivity and tight coupling problems is edge-coupled microstrip with dielectric overlays [2,3]. This configuration uses dielectric with high relative permittivity over the coupled microstrip lines to minimize the absolute difference between the even- and odd-mode phase velocities. The overlay also tightens the midband coupling compared

---

Note: Manuscript submitted August 8, 1974.

to edge-coupled microstrip without overlays. Several investigators [2,4,5] have described design methods for the dielectric overlay configuration based on design data available for edge-coupled microstrip without dielectric overlays.

This report describes a computer-aided analysis of a coupled line configuration of edge-coupled microstrip with a dielectric overlay. Design curves generated using this analysis for  $\lambda/4$  coupled line sections are presented. A discussion is presented relating to the experimental verification of the computer-aided analysis described.

## Format

The content of this report is as follows: (a) the formulation of the analysis in terms of even and odd modes is described. By virtue of a quasi-TEM model, an integro-differential equation formulation is invoked and reduced to a form suitable for use in computations. This reduction is accomplished using a method of moments solution. How to extract coupled line transmission line parameters from the reduced equations is described; (b) the computer program is documented, beginning with general considerations and proceeding with descriptions of input and output quantities. The experimental verification of the computer program is discussed; (c) design curves generated by the computer-aided analysis are described. These curves are useful for designing directional couplers, filters, and Schiffman phase shifters; (d) the results and the significance of this effort are discussed; and (e) a listing of Program MICDOC is provided in Appendix A.

## ANALYSIS

Edge-coupled microstrip with a dielectric overlay was analyzed. A quasi-TEM propagation model, used for this configuration, was characterized by a Laplacian potential cast in an integro-differential operator format. The integro-differential formulation was then reduced to matrix form by a method of moments solution. The pertinent coupled transmission line parameters were then extracted from the reduced equations. Part of the procedure used is similar to that described by Harrington, et al. [6].

### Integro-Differential Formulation

The coupled line configuration to be analyzed in this work is characterized by the admittance and phase velocities of the even and odd modes of propagation. In terms of these quantities it has been shown how to design microwave directional couplers and filters [7]. The even- and odd-mode analysis of coupled transmission line configurations transforms a 4-port coupled line problem into two 2-port transmission lines (corresponding to the even and odd modes).

The even and odd modes then correspond to "decoupled" transmission lines, each having admittances and phase velocities that can be determined as follows. Consider the cross section of the coupled line configuration shown in Fig. 1. The conducting strips A and B are photoetched on a ceramic substrate such as alumina. The dielectric overlay interfaces homogeneously with the substrate in the region between the strips and is taken to be the same material as the substrate, each characterized by relative permittivity  $\epsilon_r$ .

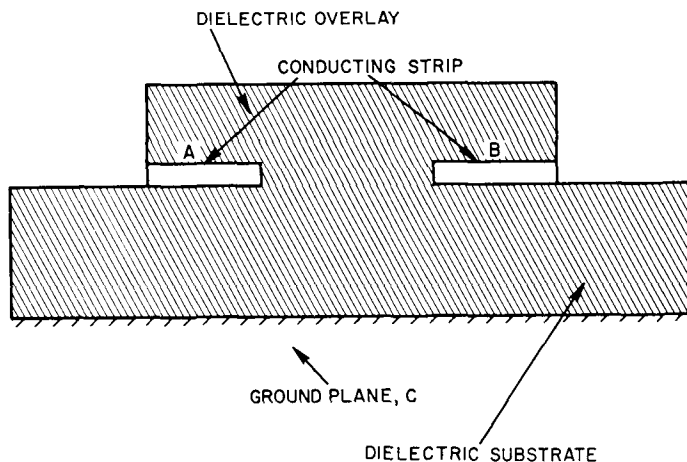


Fig. 1 — Cross section of edge-coupled microstrip with dielectric overlays (filled configuration)

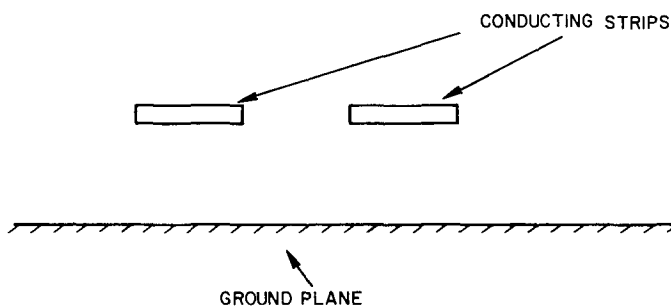


Fig. 2 — Cross section of empty configuration

The dielectric overlay precisely spans the region between the outer edges of the strips. This configuration is denoted the "filled" configuration.

Now consider the cross section shown in Fig. 2. This configuration is obtained by fictitiously removing the dielectric regions shown in Fig. 1, while retaining the same conductor geometry. The cross section in Fig. 2 is denoted the "empty" configuration.

TEM propagation models are invoked for both configurations. By virtue of these models, modal excitations are defined according to

$$\left. \begin{array}{l} \phi_A = \phi_B = 1 \\ \phi_C = 0 \end{array} \right\} \text{Even mode excitation} \quad (1)$$

$$\left. \begin{array}{l} \phi_A = -\phi_B = 1 \\ \phi_C = 0 \end{array} \right\} \text{Odd mode excitation.} \quad (2)$$

Here, the subscripts A, B, and C correspond to the conductors shown in Fig. 1. Impressing these excitations upon the filled and empty configurations produces four different scalar potential distributions. Each of these distributions can be expressed in the form

$$\phi(P) = \int_C \sigma(\ell') G(R) d\ell', \quad (3)$$

where  $\sigma(\ell')$  is a different “equivalent charge” density distribution [6] to be determined for each of the four potential distributions defined above. For a configuration composed of both conductors and dielectrics,  $\sigma$  is the sum of free and bound charges. Each distribution  $\sigma$  lies along the boundaries of conductors and dielectrics, thereby defining the integration path variable  $\ell'$ . The Green's function  $G(R)$  is the same for each of the four potential distributions and is given by

$$G(R) = \frac{1}{2\pi\epsilon_0} \ln \frac{k}{R}, \quad (4)$$

where  $R$  is the distance between the measurement point  $P$  and the charge density element at the path point determined by  $\ell'$ , contour  $C$  is the curve along which equivalent source distributions lie,  $k$  is a constant defined to assure numerical stability according to

$$k > R_{\max}, \quad (5)$$

where  $R_{\max}$  is the maximum value for  $R$  when  $P$  is constrained to lie on  $C$ ; and finally,  $\epsilon_0$  is the free-space permittivity.

At this point, the analysis approach can be summarized as follows. The four source distributions arising from the use of Eqs. (1) and (2) for the filled and empty configurations are to be determined by a method of moments solution of Eq. (3) subject to the appropriate boundary conditions for each of the four potential problems. These boundary conditions for the filled problems (even and odd modes) correspond to Eq. (1) or (2), together with the requirement for continuity of tangential electric fields at dielectric-air interfaces. For the empty configuration, even- and odd-mode problem boundary conditions are specified by Eq. (1) or (2) alone. Upon determination of the four equivalent-charge density distributions, the electrostatic capacitances  $C_e$ ,  $C_{e,e}$ ,  $C_0$ , and  $C_{e,0}$  are computed. Here  $C_e$  is the capacitance to ground per unit length of one transmission line for the filled problem with even excitation.  $C_{e,e}$  is the capacitance to ground per unit length of one line for the empty problem with even excitation.  $C_0$  and  $C_{e,0}$  are defined for the odd-mode excitation in a corresponding manner. If the inductances per unit length are taken to be the same for the filled and empty problems when considering either the even or odd mode, the modal admittances and phase velocities are evaluated according to

$$Y_{0i} = c \sqrt{C_i C_{e,i}} \quad (6)$$

and

$$v_i = c \sqrt{\frac{C_{e,i}}{C_i}}, \quad (7)$$

where

$$i = \begin{cases} e & \text{even mode} \\ 0 & \text{odd mode} \end{cases} \quad (8)$$

and  $c$  is the speed of light in free space.

The essential features of the method-of-moments solution for each of the four equivalent charge density distributions are described next.

### Method-of-Moments Reduction

To determine the equivalent-source distributions referred to earlier, Eq. (3), subject to the boundary conditions for each of the four cases described, is cast into the form

$$\alpha(\ell)\phi\Big|_{\ell} + \beta_1(\ell) \frac{\partial\phi}{\partial n_1}\Big|_{\ell} + \beta_2(\ell) \frac{\partial\phi}{\partial n_2}\Big|_{\ell} = \gamma(\ell). \quad (9)$$

Here,  $\phi|_{\ell}$  is the potential at the point on the integration path  $C$  determined by path variable value  $\ell$  as defined for Eq. (3); and  $(\partial\phi/\partial n_1)|_{\ell}$  and  $(\partial\phi/\partial n_2)|_{\ell}$  are the normal derivatives of  $\phi$  at integration path point  $\ell$  for unit normal vectors  $\vec{n}_1$  and  $\vec{n}_2$  at  $\ell$  directed to the right and left of the path, respectively, for increasing values of  $\ell$ . From this point in the development, source-position variables will be denoted by primed quantities, whereas unprimed position variables will denote potential measurement points or field points. Quantities  $\alpha(\ell)$ ,  $\beta_1(\ell)$ ,  $\beta_2(\ell)$ , and  $\gamma(\ell)$  are functions of  $\ell$  determined by the boundary conditions for each of the four potential distributions.

The method-of-moments procedure used here is described as follows. Equation (9) can be expressed succinctly as

$$L(\sigma) = \gamma, \quad (10)$$

where  $L$  is a different linear, integro-differential operator for each of the four problems at hand. An inner product for the solution is selected to be

$$\langle f, g \rangle = \int_C fg \, d\ell. \quad (11)$$

The contour  $C$  for the even- and odd-mode problems in the filled configuration is actually composed of the six contours  $C_1$  through  $C_6$  as defined in Fig. 3. Similarly, for the even- and odd-mode empty problems, the contour  $C$  is defined by the three contours,  $C_1$ ,  $C_2$ , and  $C_3$ , shown in Fig. 4. Note that contours  $C_1$ ,  $C_2$ , and  $C_3$  are the same for the filled and empty configurations. Also, each contour has constant boundary conditions in terms of the  $\alpha$ ,  $\beta_1$ ,  $\beta_2$ , and  $\gamma$  in Eq. (9).

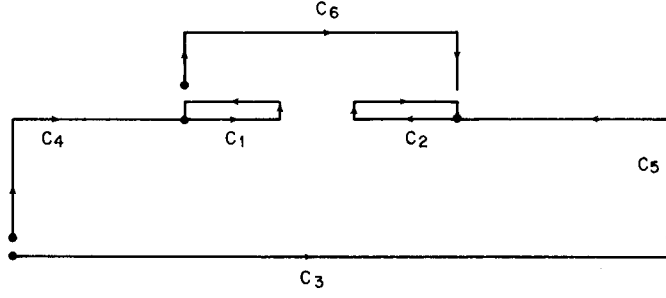


Fig. 3 — Equivalent-source representations for filled configuration

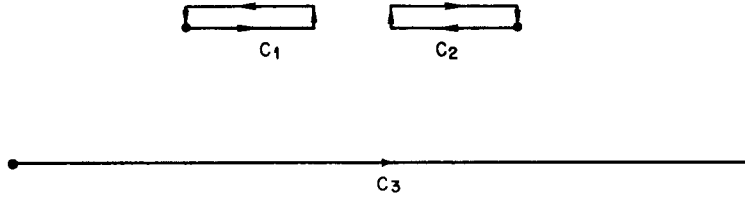


Fig. 4 — Equivalent-source representations for empty configuration

To facilitate a subsectional basis expansion for the equivalent sources in these problems, the contours  $C_1, \dots, C_6$  are subdivided into  $N_1, N_2, \dots, N_6$  subsections, respectively. The selection of  $N_1, N_2, \dots, N_6$  is determined by considering minimum numbers necessary for solution accuracy and the storage capacity of the computer to be used for this work.

The even- and odd-mode equivalent-source distributions in the filled problem are then expanded in terms of pulse functions [8] as follows:

$$\sigma_e \approx \sum_{m=1}^6 \sum_{n=1}^{N_m} \sigma_{mn}^e P_{mn} \quad (12)$$

$$\sigma_o \approx \sum_{m=1}^6 \sum_{n=1}^{N_m} \sigma_{mn}^o P_{mn}. \quad (13)$$

Here,  $\sigma_e$  and  $\sigma_o$  are the equivalent-source distributions for the filled configuration even- and odd-mode problems, respectively. Coefficients  $\sigma_{mn}^e$  and  $\sigma_{mn}^o$  are associated with the even- and odd-mode expansion functions on the  $n$ th subsection for the  $m$ th contour for the even and odd modes, respectively.  $P_{mn}$  is the pulse function on the  $n$ th subsection for the  $m$ th contour.

For the empty problem the source expansions are expressed as

$$\sigma_{e,e} \approx \sum_{m=1}^3 \sum_{n=1}^{N_m} \sigma_{mn}^{e,e} P_{mn} \quad (14)$$

and

$$\sigma_{e,0} \approx \sum_{m=1}^3 \sum_{n=1}^{N_m} \sigma_{mn}^{e,0} P_{mn}. \quad (15)$$

Here, the definitions of quantities are similar to those in the previous paragraph except that an additional superscript  $e$  is used to denote quantities for the empty configuration.

The testing procedure for the moment solution is now described. To accomplish a point-matching solution, Dirac delta functions are taken to be at the centers of the subsections defined for each of the six contours in the filled problems and the three contours in the empty problems. For each of the four problems at hand, the inner product of these impulse functions is taken according to Eq. (11), with the quantity  $\gamma$  in Eq. (10). The resulting matrix equations can be set down as

$$[\ell] [\sigma^e] = [\gamma_e] \quad (16)$$

$$[\ell] [\sigma^0] = [\gamma_0] \quad (17)$$

$$[\ell_e] [\sigma^{e,e}] = [\gamma_{e,e}] \quad (18)$$

$$[\ell_e] [\sigma^{e,0}] = [\gamma_{e,0}]. \quad (19)$$

Here,  $[\sigma^e]$  and  $[\sigma^0]$  are matrices whose elements are coefficients in the expansions shown in Eqs. (12) and (13). These elements are ordered as follows:

$$\sigma_j^e, \sigma_j^0 \quad (j = 1, \dots, N_1, N_1 + 1, \dots, N_1 + N_2, \dots, N_1 + N_2 + \dots + N_5 + 1, \dots, N_1 + \dots + N_6). \quad (20)$$

Elements of  $[\ell]$  are dependent on only geometry and material parameters and can be represented by

$$\ell_{ij} = \langle \delta_i, L(P_j) \rangle$$

$$i, j = (1, \dots, N_1, N_1 + 1, \dots, N_1 + N_2, \dots, N_1 + N_2 + \dots + N_5 + 1, \dots, N_1 + \dots + N_6) \quad (21)$$

where  $L$  is the operator in Eq. (10),  $\delta_i$  is the impulse (testing) function at the center of the  $i$ th subsection, and  $P_j$  is the pulse function on the  $j$ th subsection. Elements of the matrices  $[\gamma_e]$  and  $[\gamma_0]$  are given by

$$(\gamma_e)_i = \langle \delta_i, \gamma_e \rangle \quad (22)$$

$$(\gamma_0)_i = \langle \delta_i, \gamma_0 \rangle \quad (23)$$

where  $i$  is indexed as for Eq. (21) and  $\gamma_e$  and  $\gamma_0$  are the appropriate  $\gamma$  from Eq. (10) but specialized to the even- and odd-mode excitations, respectively, for the filled problem. The matrices  $[\sigma^{e,e}]$ ,  $[\sigma^{e,0}]$ ,  $[\ell_e]$ ,  $[\gamma_{e,e}]$ , and  $[\gamma_{e,0}]$  are defined in a manner completely analagous to  $[\sigma^e]$ ,  $[\sigma^0]$ ,  $[\ell]$ ,  $[\gamma^e]$ , and  $[\gamma^0]$  except that they correspond to the empty problem and the indices  $i$  and  $j$  are ordered

$$i, j (1, \dots, N_1, N_1 + 1, \dots, N_1 + N_2, N_1 + N_2 + 1, \dots, N_1 + N_2 + N_3). \quad (24)$$

Explicit representations for elements of matrices  $[\ell]$  and  $[\ell_e]$  are virtually the same as elements of matrix  $[\ell_{ji}]$  in Ref. 6.

The solution for the coefficients from the equivalent-source expansion in Eqs. (12) through (15) is achieved by inverting the  $[\ell]$  and  $[\ell_e]$  matrices in Eqs. (16) through (19). Hence,

$$[\sigma^e] = [\ell]^{-1} [\gamma_e] \quad (25)$$

$$[\sigma^0] = [\ell]^{-1} [\gamma_0] \quad (26)$$

$$[\sigma^{e,e}] = [\ell_e]^{-1} [\gamma_{e,e}] \quad (27)$$

$$[\sigma^{e,0}] = [\ell_e]^{-1} [\gamma_{e,0}]. \quad (28)$$

Using the coefficients determined according to Eqs. (25)-(28) and Eqs. (12)-(15), respectively, produces step approximations to the equivalent-source distributions.

In the next section it is shown how to determine the even- and odd-mode transmission line parameters from the approximations to the equivalent-source distributions, represented according to Eqs. (12)-(15).

### Determination of Even- and Odd-Mode Transmission Line Parameters

Here, equivalent-source distributions obtained using Eqs. (25)-(28) are used to determine the even- and odd-mode transmission line impedances, phase velocities, and other quantities pertinent to the design of coupled line components.

The capacitances  $C_e$ ,  $C_0$ ,  $C_{e,e}$ , and  $C_{e,0}$ , described on page 4 are determined. Each capacitance is defined by the ratio of net free charge to impressed voltage for the even- or odd-mode transmission lines in the filled or empty configurations, respectively. Hence,

$$C_e = \frac{(Q_e)}{\phi_A} \quad (29)$$

$$C_0 = \frac{(Q_0)}{\phi_A} \quad (30)$$

$$C_{e,e} = \frac{(Q_{e,e})}{\phi_A} \quad (31)$$

$$C_{e,0} = \frac{(Q_{e,0})}{\phi_A}, \quad (32)$$

where  $Q_e$  and  $Q_0$  are the net free charge on one of the coupled strips for the filled configuration under the excitations in Eqs. (1) and (2), respectively. Similarly,  $Q_{e,e}$  and  $Q_{e,0}$  in Eqs. (31) and (32) are defined for the empty configurations with the even- and odd-mode excitations impressed according to Eqs. (1) and (2).

The determination of the net free charges  $Q_e$ ,  $Q_0$ ,  $Q_{e,e}$ , and  $Q_{e,0}$  is based on the assumption that the conductors in the problem are perfect. Hence, there are no fields internal to the conductors. Upon applying Gauss's Law we can write the expressions

$$Q_e \approx \epsilon_0 \sum_{j=1}^{N_1} \epsilon_{rj} \sigma_j^e \Delta \ell'_j, \quad (33)$$

$$Q_0 \approx \epsilon_0 \sum_{j=1}^{N_1} \epsilon_{rj} \sigma_j^0 \Delta \ell'_j, \quad (34)$$

$$Q_{e,e} \approx \epsilon_0 \sum_{j=1}^{N_1} \sigma_j^{e,e} \Delta \ell'_j, \quad (35)$$

and

$$Q_{e,0} \approx \epsilon_0 \sum_{j=1}^{N_1} \sigma_j^{e,0} \Delta \ell'_j \quad (36)$$

where  $\sigma_j^e$ ,  $\sigma_j^0$ ,  $\sigma_j^{e,e}$ , and  $\sigma_j^{e,0}$  are defined as per Eqs. (11)-(19);  $\Delta \ell'_j$  is the length of the  $j$ th segment into which contours  $C_1$  in Figs. 3 and 4 are subdivided; and  $\epsilon_{rj}$  is the relative permittivity of the medium immediately adjacent to the  $j$ th segment and outside the conducting strip bounded by contour  $C_1$ . Since the potential  $\phi_A$  in Eqs. (1) and (2) is equal to unity,

$$C_e \approx \epsilon_0 \sum_{j=1}^{N_1} \epsilon_{rj} \sigma_j^e \Delta \ell'_j, \quad (37)$$

$$C_0 \approx \epsilon_0 \sum_{j=1}^{N_1} \epsilon_{rj} \sigma_j^0 \Delta \ell'_j, \quad (38)$$

$$C_{e,e} \approx \epsilon_0 \sum_{j=1}^{N_1} \sigma_j^{e,e} \Delta \ell'_j, \quad (39)$$

and

$$C_{e,0} \approx \epsilon_0 \sum_{j=1}^{N_1} \sigma_j^{e,0} \Delta \ell'_j. \quad (40)$$

Using Eqs. (37)-(40) with Eqs. (6) and (7), we can determine the even- and odd-mode admittances  $Y_{0e}$  and  $Y_{0o}$  and the phase velocities for the coupled line configuration in Fig. 1.

Other pertinent coupled transmission line parameters can be computed as follows. The even- and odd-mode impedances are given by

$$Z_{0i} = \frac{1}{Y_{0i}} \quad i = \begin{cases} e & \text{even mode} \\ o & \text{odd mode.} \end{cases} \quad (41)$$

The coupled line impedance is given by

$$Z_0 = \sqrt{Z_{0e} Z_{0o}} \quad (42)$$

where  $Z_{0e}$  and  $Z_{0o}$  are evaluated according to Eq. (41). In some cases the average  $v_{\text{avg}}$  of the even- and odd-mode phase velocities is of interest as a measure of the phase delay for coupled-mode propagation. Velocity  $v_{\text{avg}}$  is expressed simply as

$$v_{\text{avg}} = \frac{v_e + v_o}{2}. \quad (43)$$

Finally, for the analysis of directional couplers composed of sections of coupled lines with the cross-sectional configuration shown in Fig. 1, the midband voltage coupling coefficient  $C_0$  is given by

$$C_0 = \frac{\frac{Z_{0e}}{Z_{0o}} - 1}{\frac{Z_{0e}}{Z_{0o}} + 1}, \quad (44)$$

where  $Z_{0e}$  and  $Z_{0o}$  are evaluated according to Eq. (41) in the preceding discussion.

## COMPUTER PROGRAM

The described analysis has been implemented in the form of a versatile digital computer program. Here, the usage of this program from the standpoint of a design engineer as the user is described. A complete listing of this computer program is presented in Appendix A.

## General Considerations

The computer program is named MICDOC, an acronym derived from the phrase, "microwave integrated circuit dielectric overlay couplers." MICDOC is written in Fortran IV and is compatible with the CDC 3800 digital computer. With minor alterations this program should also be suitable for use on the CDC 6000 series computer systems and the IBM 360 or 370 systems. The core storage necessary for executing this program on the CDC 3800 system at the Naval Research Laboratory (NRL) Research Computation Center is 41,648 words. Although the total core storage of this computer is now 98,304 words, the maximum storage available for a single array (without resorting to special array-handling techniques) is 37,768 words. It is this system requirement that constrains the largest array in MICDOC to be  $181 \times 181$  or 37,761 words.

Furthermore, because of the standard loading procedure employed by the CDC 3800 system at NRL, the following scheme for handling large arrays was incorporated into MICDOC. The two relatively large arrays in MICDOC are array A,  $181 \times 181$ , and array A1,  $132 \times 132$ . These arrays appear in different subroutines and are used successively. For these reasons the arrays A and A1 are placed in a block of COMMON storage labeled HELP. During the loading of the program, HELP is loaded into a storage bank with 37,768 storage addresses available to accommodate array A. This is done using a BANK card. In addition, another BANK card forces main Program MICDOC and Subroutine MSCUPF into a different storage bank. The storage required to operate using A and A1 is minimized by forcing them to share the same storage locations by means of the statement, EQUIVALENCE (A, A1). These techniques are necessary to load properly program MICDOC into the CDC 3800 system at NRL.

The length of time necessary for program execution is approximately 6 min for each configuration to be analyzed.

## Input Information

An understanding of the input quantities required by Program MICDOC is facilitated by considering the geometry displayed in Fig. 5. Each configuration of edge-coupled microstrip with a dielectric overlay to be analyzed by MICDOC can be characterized by specifying the cross section in terms of quantities defined in Fig. 5. Accordingly, the first data card for any execution of MICDOC contains the quantity NSETS. This is an integer specifying the number of different configurations of the type defined by Fig. 5 which are to be analyzed. NSETS is punched on the first data card according to the format I10.

Each configuration included in NSETS is specified by a separate data card located successively behind the first card. Each card lists the following quantities, defined in Fig. 5 and punched according to the format F10.6:

- W* The width of a conducting strip, specified in mils
- S* The spacing between the two conducting strips, specified in mils
- T* The thickness of the dielectric overlay above the top surface of the conducting strips, specified in mils

- H* The height of the conducting strips above the ground plane (the substrate thickness), specified in mils
- L* The substrate width, specified in inches. This quantity is variable primarily to allow for narrow substrate widths. A value of  $L = 1.0$  in. has been adequate for many practical coupler circuits.
- ER* The relative dielectric constant of the substrate and dielectric overlay (dimensionless).

The number of cards behind the first card, each containing sets of the parameters described above, should equal the value read in for NSETS.

### Output Information

An understanding of the output information furnished by Program MICDOC is facilitated by examining a sample of the program output. Such a sample is shown in Fig. 6. The output in this figure corresponds to an input data set, where

$$NSETS = 1$$

$$W = 47.5 \text{ mils}$$

$$S = 61.0 \text{ mils}$$

$$T = 65.0 \text{ mils}$$

$$H = 50.0 \text{ mils}$$

$$L = 1.0 \text{ in.}$$

$$ER = 10.0.$$

The parameters following NSETS are those defined in Fig. 5.

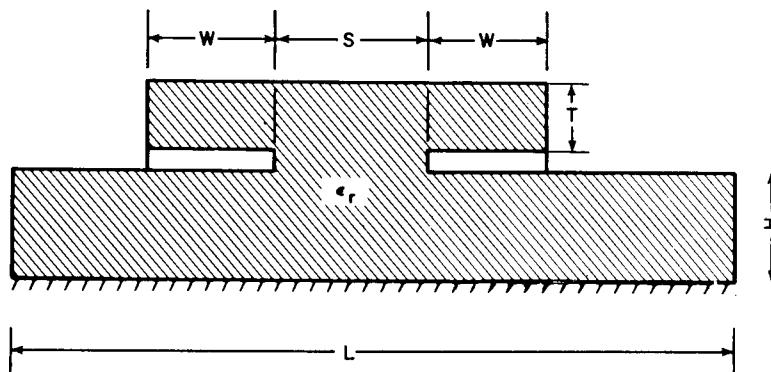


Fig. 5 — Input parameters required by Program MICDOC

```

STRIP METALIZATION THICKNESS = 250 MICRONS
W = 47.5   S = 61.0   T = 65.0   H = 50.0   L = 1.000000   ER = 10.000000
C(DB)      ZO(OHMS)  ZOO(OHMS)  ZOE(OHMS)  VO(M/SEC)  VE(M/SEC)  VAVG(M/SEC)
14.66      43.85     36.37     52.87     1.007+008  1.066+008  1.036+008
CO(PF) = 273.180   CE(PF) = 177.494   CEO(PF) = 30.755   CEE(PF) = 22.395

```

Fig. 6 — Output sample from Program MICDOC for input parameters:  $NSETS = 1$ ,  $W = 47.5$ ,  $S = 61.0$ ,  $T = 65.0$ ,  $H = 50.0$ ,  $L = 1.0$ ,  $ER = 10.0$

The corresponding output shown in Fig. 6 is described as follows. The first line of output is invariant for each configuration and indicates that the computer program performs computations taking the strip conductors to have a nonzero metalization thickness of 250  $\mu\text{in}$ . The next line is skipped, and the third line lists the input parameters, defined according to Fig. 5, for the configuration to be analyzed. After skipping another line, the program tabulates the following computed quantities from left to right with identifying labels printed directly above computed values.

$C(\text{DB})$ : The computed value of midband coupling in dB, determined using Eq. (44)

$ZO(\text{OHMS})$ : The coupled line characteristic impedance in ohms, computed using Eq. (42)

$ZOO(\text{OHMS})$ ,  $ZOE(\text{OHMS})$ : The odd- and even-mode impedances, respectively, in ohms, evaluated as described leading to Eq. (41)

$VO(\text{M/SEC})$ ,  $VE(\text{M/SEC})$ : The odd- and even-mode phase velocities, respectively, in meters per second, determined as described earlier in the analysis, using Eq. (7).

$VAVG(\text{M/SEC})$ : The average of the even- and odd-mode phase velocities in meters per second, computed using Eq. (43).

Another line is skipped and the last line in the output block lists from left to right the quantities  $CO(PF)$ ,  $CE(PF)$ ,  $CEO(PF)$ , and  $CEE(PF)$ , which are the capacitances (in picofarads) evaluated according to Eqs. (38), (37), (40), and (39), respectively.

For program executions where more than one configuration is to be analyzed ( $NSETS > 1$ ), an output block similar to the one shown in Fig. 6 is printed for each configuration. Four blank lines separate the output information blocks printed for each configuration.

### Experimental Verification of Program MICDOC

Although Program MICDOC provides information that is suitable for use in developing directional filters and Schiffman phase shifters, the program was implemented initially for use in developing broadband directional couplers. Therefore, much of the data currently available for use in assessing the accuracy of MICDOC is constituted of laboratory

measurements made on two-section, asymmetric, directional couplers. These couplers have sections of coupled lines embodying the configuration treated here.

For the purpose of verifying the accuracy of the computer program, the measured performance of three of these directional couplers will be compared with computer-evaluated performance characteristics. The design of these couplers used computations obtained from MICDOC. One of these couplers has a nominal coupling value of 10 dB and is shown in Fig. 7. Depicted in this figure is the coupler circuit pattern, which was fabricated on a  $0.9 \times 0.4 \times 0.025$ -in. alumina substrate using photolithographic fabrication techniques. The dielectric overlay for each of the parallel-coupled line regions was formed by affixing precisely ground pieces of alumina to the surface of the appropriate coupled strip region using Emerson and Cumings Stycast *HiK* ( $K = 10$ ) Epoxy. These dielectric pieces are shown in Fig. 7, both separately and affixed to couplers packaged for experimental evaluation. Each of the two sections of this coupler has a cross-sectional configuration of the type shown in Fig. 5 with the characterizing parameters shown in Table 1.

The accuracy of MICDOC in describing the performance of this coupler is determined as follows. By applying MICDOC to the two coupled line cross sections defined in Table 1, we determine that the midband coupling values of the tight and loose sections are 7.0 dB and 16.1 dB, respectively. The characteristic impedance of each of these coupled line regions is evaluated to be 50 ohms. Using an ABCD matrix description [1] for the two-section coupler, we evaluated the performance of the two-section coupler. The performance computed in this manner was compared with the measured performance characteristics, shown in Fig. 8, for the packaged coupler shown in Fig. 7. Since the performance

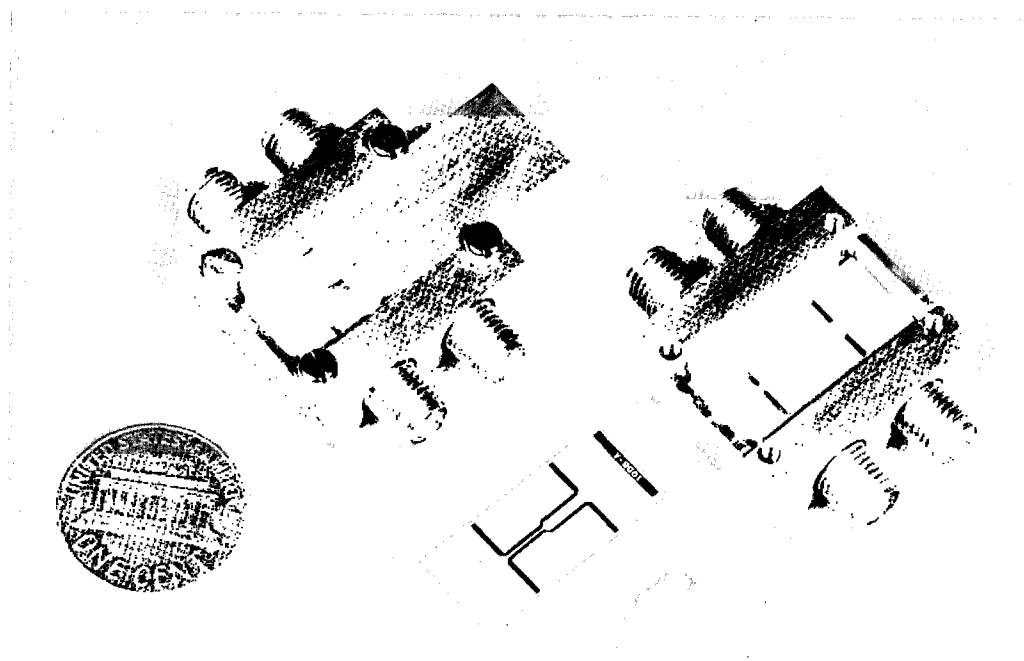


Fig. 7 — Photograph of 10-dB coupler and package assembly

Table 1  
Cross-Sectional Parameters for Two-Section 10-dB Coupler

Section	Parameter					
	<i>W</i> (Mils)	<i>S</i> (Mils)	<i>T</i> (Mils)	<i>H</i> (Mils)	<i>L</i> (In.)	<i>ER</i>
Tightly coupled	15.7	5.2	4.5	25.0	1.0	10.0
Loosely coupled	20.0	30.4	6.5	25.0	1.0	10.0

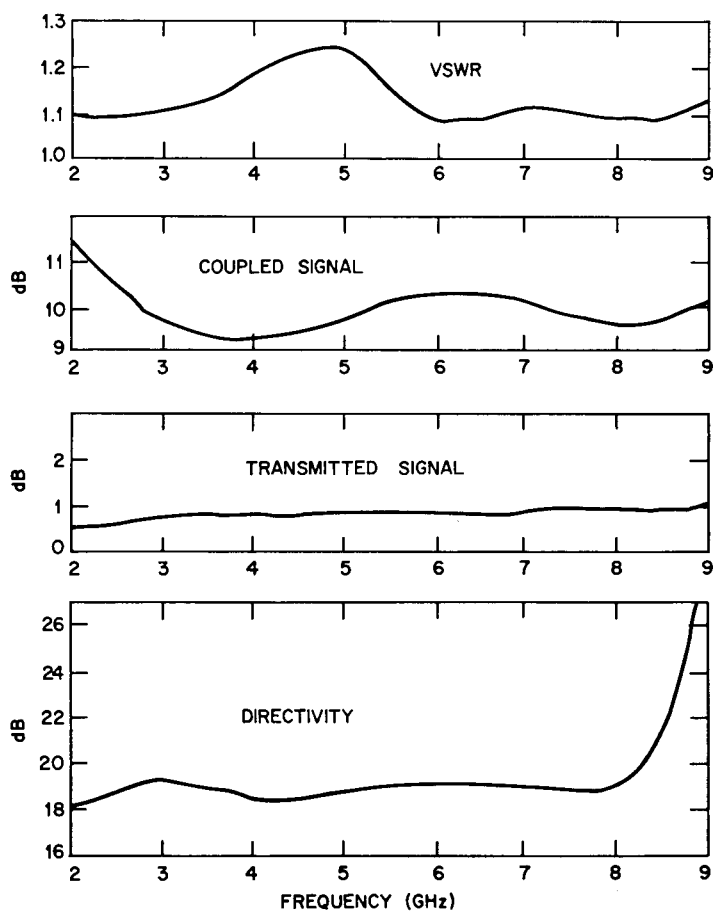


Fig. 8 — Measured performance of 10-dB coupler

determined by MICDOC assumes that there are no dissipation losses, the most direct assessment of the program accuracy is made by eliminating the measured dissipation loss effects from the measured coupling characteristic shown in Fig. 8. When this is done, it is found that, for the frequency range from 2.5 to 8.5 GHz, the computed and loss-adjusted coupling characteristics are each  $9.6 \pm 0.6$  dB. The input VSWR characteristic shown in Fig. 8 includes the effects of mismatches from SMA connectors, transitions from connectors into microstrip lines, and the right-angle mitred bends leading to the coupled line sections. In spite of these contributions, the worst-case input VSWR for the 2.5- to 8.5-GHz region is 1.25:1, indicating substantial agreement between computed and actual impedance levels for the two sections. The coupled line regions of each section were each 0.2 in. long in the experimental coupler model. Using MICDOC the average phase velocity (Eq. (43)) for each section was computed to be  $1.1 \times 10^8$  m/s. From this value the midband frequency is evaluated to be 5.4 GHz. This value agrees closely with the measured characteristics in Fig. 8. Specifically, the computed midband frequency of 5.4 GHz is only 1.8% different compared to 5.56 GHz, the center of the 2.5- to 8.5-GHz frequency band for which the measured characteristic was cited earlier. It should be noted, however, that the midband frequency value for the data in Fig. 8 is not precisely determinable.

Another two-section coupler, which provides information for investigating the accuracy of MICDOC, is nominally a 6.7-dB coupler. With regard to fabrication and design techniques employed, this coupler is very similar to the 10-dB coupler just described. However, the microstrip line widths, spacings, and overlay geometries used in the two cascaded sections differ from those used in the 10-dB coupler. Table 2 gives the parameters for the tightly and loosely coupled sections of the experimental 6.7-dB coupler model. Measured performance characteristics for this coupler are shown in Fig. 9. These coupler sections were computed to have midband coupling values of 4.0 dB and 13.2 dB, respectively. The characteristic impedances of these sections were evaluated to be 50 ohms. The computed average value of phase velocity for each section is again  $1.1 \times 10^8$  m/s. Comparing computed with measured performance characteristics for this coupler in a manner similar to that used for the 10-dB coupler, we note that for the 2.5- to 8.5-GHz range the computed coupling is  $6.1 \pm 0.4$  dB compared to  $6.3 \pm 0.6$  dB measured. The measured VSWR over the same frequency range is 1.28:1 or better and includes effects of reflections from connectors and mitred bends. Since the coupler sections are each 0.2 in. long, the computed midband frequency is 5.4 GHz. This compares favorably with the observed midband frequency for measured performance of approximately 5.5 GHz.

A third two-section coupler that is useful for evaluating the accuracy of MICDOC is nominally a 20-dB coupler. The construction of this coupler is similar to that shown in Fig. 7 for the 10-dB coupler. The characteristics of the cross sections employed in this coupler are given in Table 3. The measured performance for this coupler is displayed in Fig. 10. These coupler sections were evaluated as having midband coupling values of 16.9 dB and 27.1 dB, respectively. The characteristic impedances of these sections were evaluated to be 50 ohms. The computed average value of phase velocity for both sections is  $1.05 \times 10^8$  m/s. Comparing computed with measured performance characteristics for this coupler in a manner similar to those used for the 10-dB and 6.7-dB couplers shows that for the 2.5- to 8.5-GHz range the computed coupling is  $19.6 \pm 0.5$  dB compared to  $20.35 \pm 0.35$  dB measured. The measured VSWR over the same frequency range is 1.23:1 or better and includes effects of reflections from connectors and mitred bends. Since the coupler sections are each 0.2 in. long, the computed midband frequency is 5.2 GHz.

Table 2  
Cross-Sectional Parameters for Two-Section 6.7-dB Coupler

Section	Parameter					
	<i>W</i> (Mils)	<i>S</i> (Mils)	<i>T</i> (Mils)	<i>H</i> (Mils)	<i>L</i> (In.)	<i>ER</i>
Tightly coupled	7.8	2.1	10.0	25.0	1.0	10.0
Loosely coupled	20.6	19.2	5.0	25.0	1.0	10.0

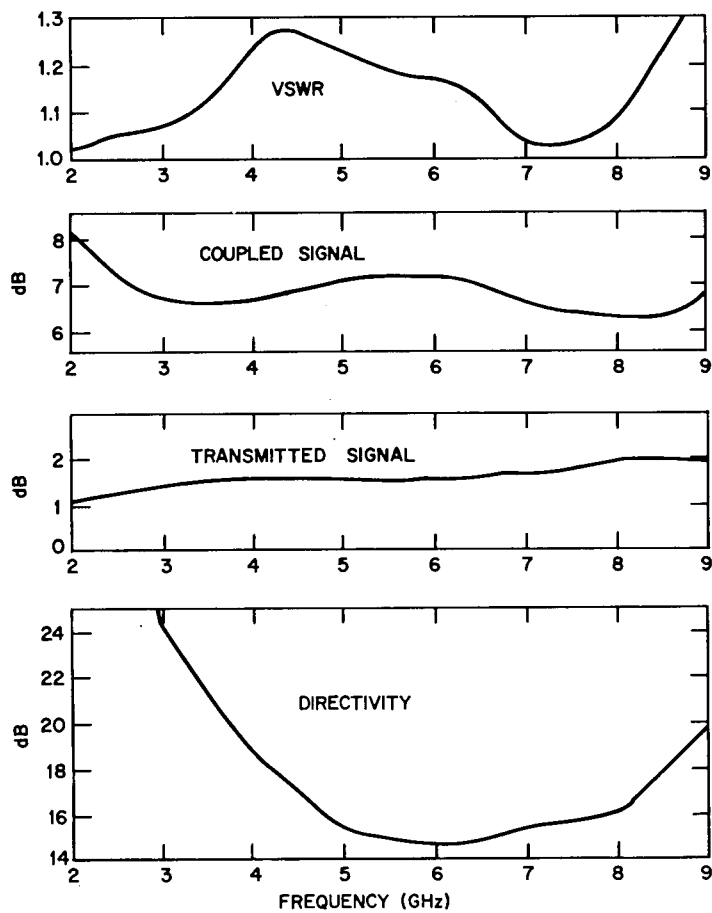


Fig. 9 — Measured performance of 6.7-dB coupler

Table 3  
Cross-Sectional Parameters for Two-Section 20-dB Coupler

Section	Parameter					
	$W$ (Mils)	$S$ (Mils)	$T$ (Mils)	$H$ (Mils)	$L$ (In.)	$ER$
Tightly coupled	18.8	39.6	25.0	25.0	1.0	10.0
Loosely coupled	18.5	85.5	25.0	25.0	1.0	10.0

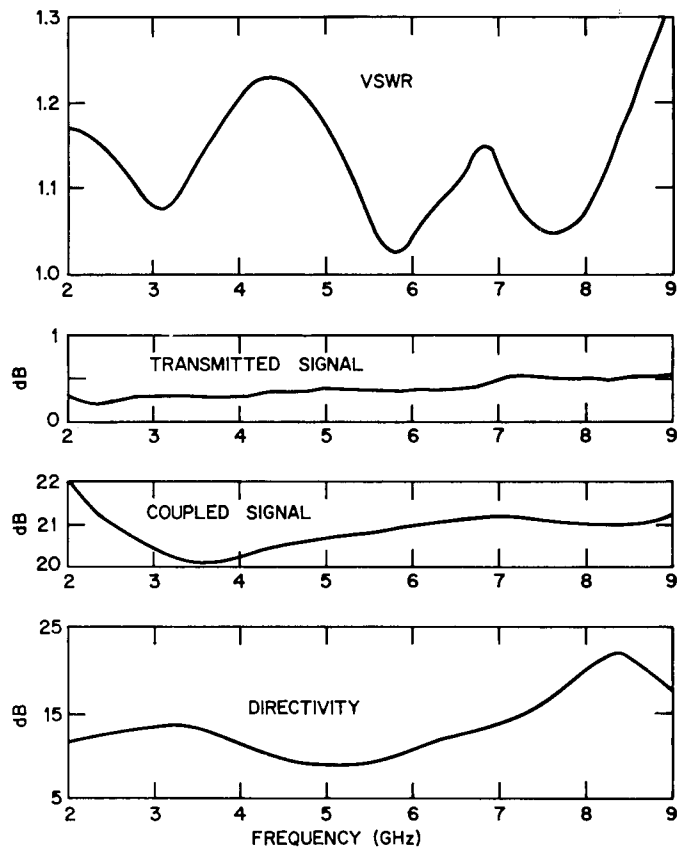


Fig. 10 — Measured performance of 20-dB coupler

Table 4  
Values of Midband Coupling for Configurations Used in  
Experimental Configuration of Program MICDOC

Midband Coupling (dB)
4.0
7.0
13.2
16.1
16.9
27.1

Based on the periodicity observed in the measured coupling characteristic at frequencies through 12 GHz (not shown in Fig. 10), the measured midband frequency for this coupler occurs at approximately 5.6 GHz. It should be noted that the poorer worst-case directivity for the data in Fig. 10, compared to those shown in Figs. 8 and 9 is not due to computational error in MICDOC. Instead, this is because the 20-dB coupler was not optimized with respect to directivity [3], as were the 10-dB and 6.7-dB couplers.

By comparing computed with measured performance for 10-, 6.7-, and 20-dB two-section couplers, we have demonstrated the utility of program MICDOC for a wide range of coupling. Table 4 lists the values of midband coupling corresponding to the six sections utilized in these three couplers. The comparisons of computed with measured performance for the three broadband couplers have confirmed that the accuracy of Program MICDOC is sufficient for many design applications.

## DESIGN CURVES

Although the utility of the computer program has been demonstrated in the preceding paragraphs the information generated by this program can be put into a format that is yet more suitable for use in designing directional couplers, filters, and Schiffman phase shifters. The desirability of such a format is illustrated by the following example. Suppose it is desired to determine those parameters for the configuration shown in Fig. 5 that will lead to a coupled line section with midband coupling of  $C(\text{dB})$  and a coupled line characteristic impedance  $Z_0$  ohms. This typifies the design problem encountered in prescribing the sections necessary for the experimental 10-, 6.7-, and 20-dB couplers described earlier. To use program MICDOC for such applications requires an initial guess at the appropriate values for the parameters in Fig. 5. Upon obtaining calculations from one initial application of MICDOC, successive judicious modifications of the parameters and program applications are usually necessary to determine those parameters necessary for sufficiently accurate values of  $C(\text{dB})$  and  $Z_0$  ohms. Typically, three applications of MICDOC have been adequate to determine values of  $C(\text{dB})$  and  $Z_0$  ohms with an error of approximately 3%.

To reduce the effort necessary for using the analysis to design directional couplers, filters, and Schiffman phase shifters, MICDOC has been used to generate several families

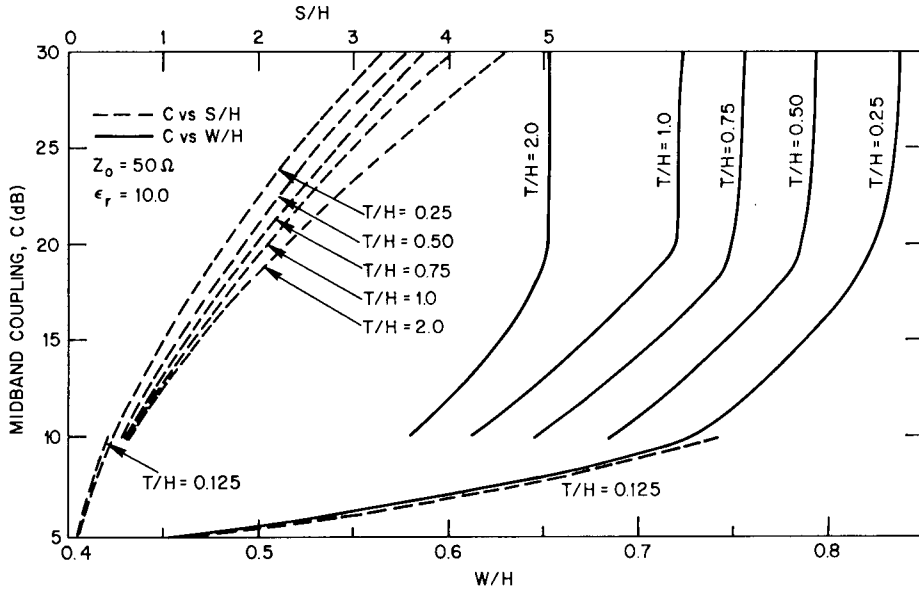


Fig. 11 — Midband coupling vs normalized strip width and spacing for values of normalized overlay thickness

of design curves. Figure 11 shows plots of midband coupling in decibels vs both normalized strip width ( $W/H$ ) and spacing ( $S/H$ ) for values of normalized overlay thickness ( $T/H$ ) from  $T/H$  equal to 0.25 through 2.00. Notation used here is defined in Fig. 5. Midband coupling values are shown in the range from 5 through 30 dB. These curves are intended for providing geometry necessary to achieve a value of characteristic impedance  $Z_0$  equal to 50 ohms using dielectric substrates and overlays with  $\epsilon_r$  equal to 10.0. To determine the configuration, of the type shown in Fig. 5, that will produce a value of midband coupling  $C$ (dB) and a characteristic impedance of 50 ohms, first a value of  $T/H$  is determined. This is done as described in Ref. 3. Once a value of  $T/H$  is selected the value of  $W/H$  is determined from Fig. 11 by reading horizontally from the proper value of  $C$ (dB) to the solid curve with the prescribed value of  $T/H$ . Reading down from this point to the scale for  $W/H$  produces the necessary value of normalized strip width. Using a similar procedure with the family of broken curves and reading up to the scale for  $S/H$  completes the configuration characterization, while assuring a 50-ohm characteristic impedance.

Other design curves presented, which are used in the manner described for Fig. 11, are as follows. Figures 12 and 13 present values of even- and odd-mode impedance ( $Z_{0e}$  and  $Z_{0o}$ ) vs  $W/H$  and  $S/H$  for various values of  $T/H$ . Figures 14 and 15 present values of even- and odd-mode phase velocity ( $v_e$  and  $v_o$ ) vs the same parameters. Figure 16 presents  $v_{avg}$  against the same parameters. Figures 11 through 16 all yield configurations of edge-coupled microstrip with a dielectric overlay having a characteristic impedance of 50 ohms for dielectric material with  $\epsilon_r$  equal to 10.0.

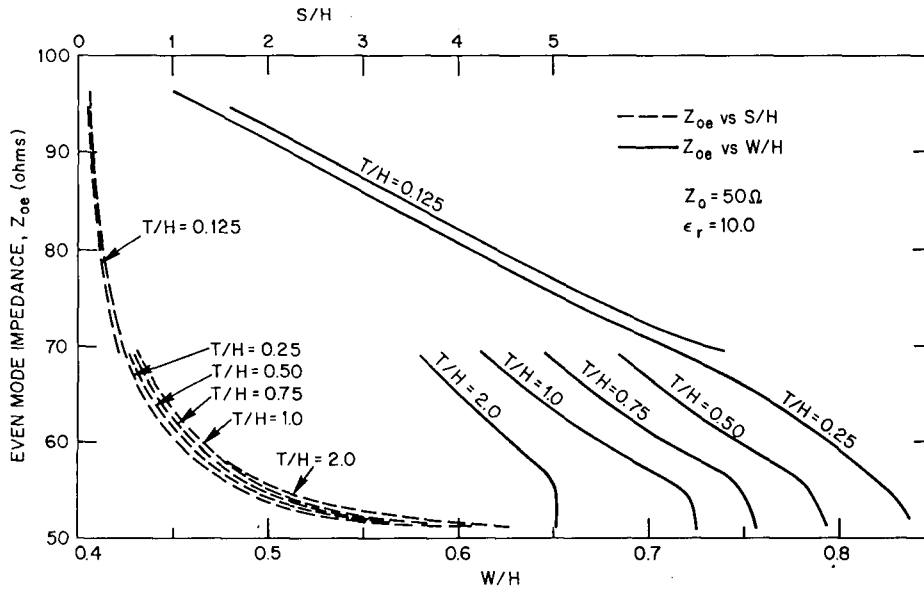


Fig. 12 — Even-mode impedance vs normalized strip width and spacing for values of normalized overlay thickness

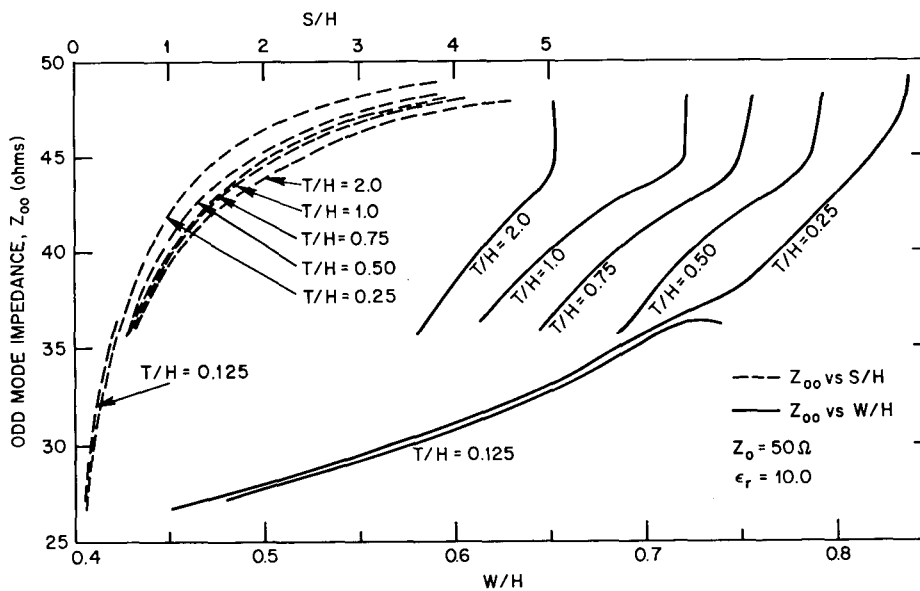


Fig. 13 — Odd-mode impedance vs normalized strip width and spacing for values of normalized overlay thickness

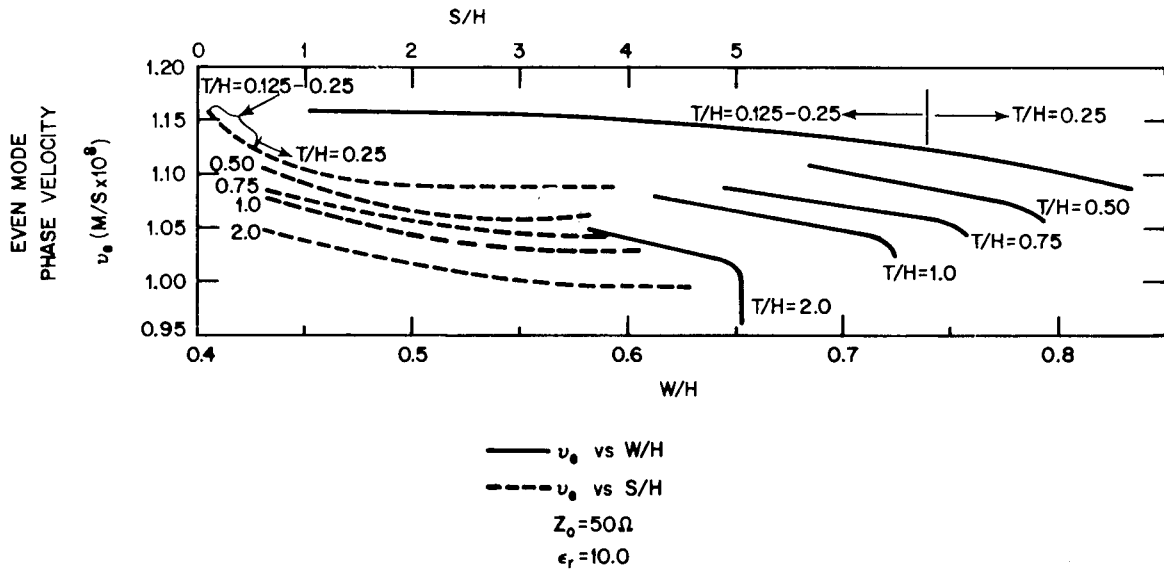


Fig. 14 — Even-mode phase velocity vs normalized strip width and spacing for values of normalized overlay thickness

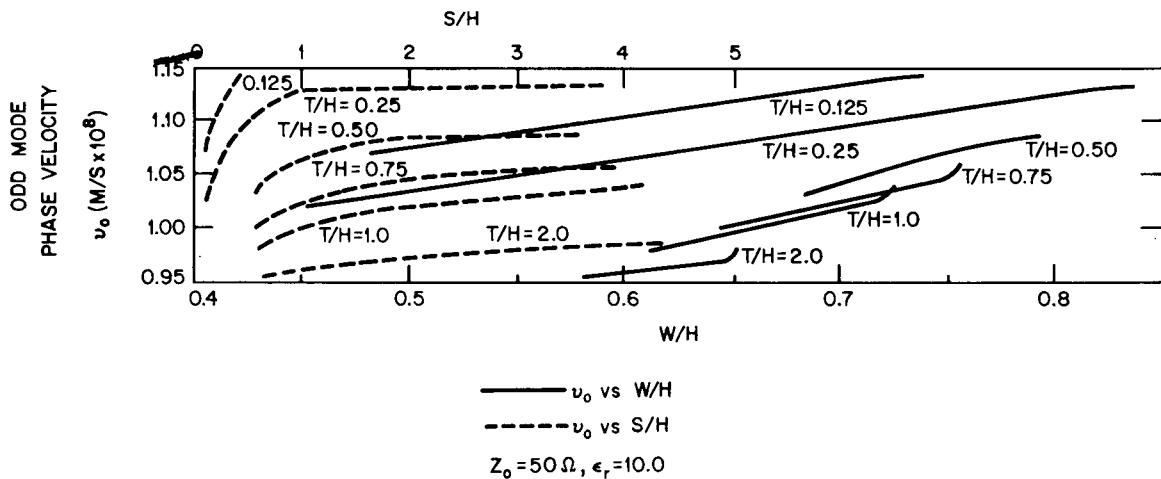


Fig. 15 — Odd-mode phase velocity vs normalized strip width and spacing for values of normalized overlay thickness

## DISCUSSION

This report describes a computer-programmed analysis and design curves useful for determining the propagation characteristics of electromagnetic waves along coupled microstrip lines with dielectric overlays. Computations made using the computer program have been compared with experimental results and were found to be in error by less than 5% and typically 3% for midband coupling, modal impedances, and coupled line impedance values. Based on the similarity of the coupled line configuration treated here with that described by Krage and Haddad [9], it is anticipated that the modal and coupled line phase velocities in this work are more dispersive than the modal and coupled line impedance quantities. Because of the quasi-TEM propagation model employed in this analysis,

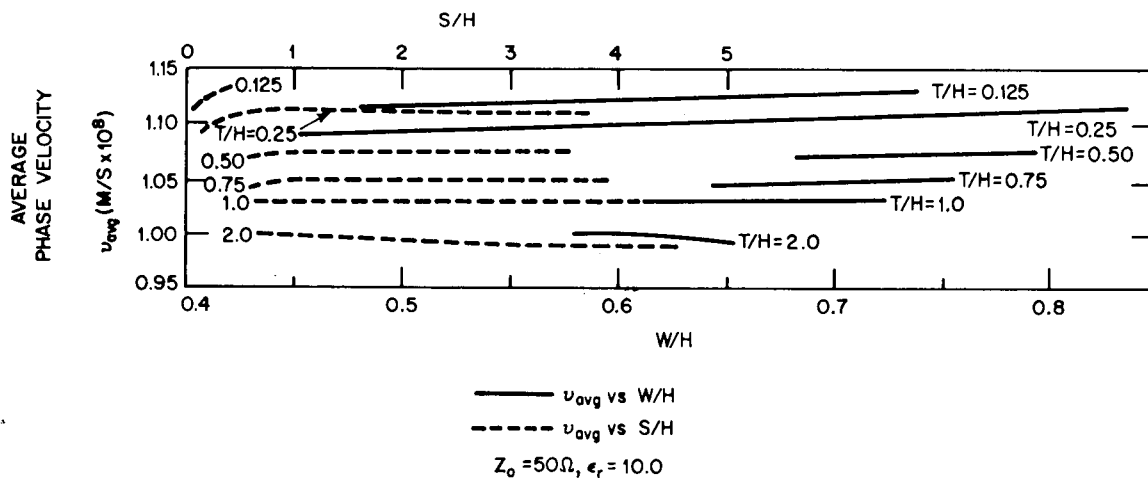


Fig. 16 — Average phase velocity vs normalized strip width and spacing for values of normalized overlay thickness

it is to be expected that phase velocity computations will, in general, incur slightly greater errors than the impedance calculations. Errors in phase velocity calculations are probably on the order of 5%.

The design curves shown in Figs. 11 through 16 are expected to yield coupled line characteristics with essentially the same accuracy as that described in the preceding paragraph. The values in these curves have been found to be consistent with measured electrical characteristics of the two-section couplers composed of the coupling values in Table 4.

Program MICDOC currently comprises the only computer-aided analysis that has been developed and distributed specifically to treat coupled microstrip *with a* dielectric overlay. There have been other investigations producing design information for similar configurations [4,5,9]. However, the efforts of Lee [4] and Buntschuh [5] consist of empirical modifications of computer-generated analysis data for edge-coupled microstrip *without* dielectric overlays (Bryant and Weiss [10]). These approaches are not as convenient for design purposes as the single tool Program MICDOC. Furthermore, the use of the analysis developed here can lead to a more general, systematic design procedure for developing broadband directional couplers, filters, and Schiffman phase shifters [3], allowing for the independent design of  $\lambda/4$  coupled line sections. The effort by Krage and Haddad [9] did not lead to a generally available analysis for coupled microstrip overlay configurations. Also, the overlay configuration treated in that work offers considerably greater difficulty in achieving a well-matched transition at ports where coupled lines interface with isolated microstrip lines.

## ACKNOWLEDGMENT

The author extends his sincere thanks to Max L. Reuss, Jr., for his valuable comments and suggestions during this work and to Boris Sheleg for his contributions to the experimental portion of this effort. Special thanks go to Mrs. Flosada Huff for typing the manuscript.

1. L. Young, editor, *Advances in Microwaves*, vol. 1, Academic Press, Inc., New York, 1966.
- ✓ 2. B. E. Spielman, "The Development of a 20 dB Multi-Octave Directional Coupler for MIC Applications," Late Paper, *1973 IEEE-GMTT International Microwave Symposium*, Boulder, Colo., June 4-6, 1973.
- ✓ 3. B. Sheleg, and B. E. Spielman, "Broadband Directional Couplers Using Microstrip with Dielectric Overlays," Late Paper, *1974 IEEE S-MTT International Microwave Symposium*, Atlanta, Ga., June 12-14, 1974.
- ✓ 4. Y. S. Lee, "Mode Compensation Applied to Parallel-Coupled Microstrip Directional Filter Design," *IEEE Trans. MTT-22*, 66-69, (Jan. 1974).
- ✓ 5. C. Buntschuh, "Octave-Bandwidth Microstrip," RADC-TR73-396, Rome Air Development Center, Rome, N.Y., Contract F30602-72-C-0282, Jan. 1974. AD 777320
6. R. F. Harrington, et al., "Computation of Laplacian Potentials by an Equivalent Source Method," *Proc. IEE*, 116, No. 10, 1715-1720, (Oct. 1969).
7. G. L. Matthaei, L. Young, and E. M. T. Jones, *Microwave Filters, Impedance-Matching Networks, and Coupling Structures*, McGraw-Hill, New York, 1964.
8. R. F. Harrington, *Field Computation by Moment Methods*, Macmillan Co., New York, 1968.
9. M. K. Krage, and G. I. Haddad, "Frequency-Dependent Characteristics of Microstrip Transmission Lines," *IEEE Trans. MTT-20*, 678-688, (Oct. 1972).
10. T. G. Bryant, and J. A. Weiss, "Parameters of Microstrip Transmission Lines and of Coupled Pairs of Microstrip Lines," *IEEE Trans. MTT-16*, 1021-1027, (Dec. 1968).

# Appendix A LISTING OF PROGRAM MICDOC

```

PROGRAM MICDOC
REAL L
READ 1, NSETS
1 FORMAT(I10)
DO 2 MN=1,NSETS
  READ 3,W,S,T,H,L,ER
3 FORMAT(6F10.6)
  PRINT 8
8 FORMAT(1H ,////1H ,*STRIP METALIZATION THICKNESS = 250 MICROINCHES
1*)
  PRINT 4,W,S,T,H,L,ER
4 FORMAT(1H0,2HW=,F5.1,3X,2HS=,F5.1,3X,2HT=,
1F5.1,3X,2HH=,F5.1,3X,2HL=,F10.6,3X,3HER=,F10.6)
  FACTOR=(1.0E-05)*(1./0.393700)
  W=W*FACTOR
  S=S*FACTOR
  T=T*FACTOR
  H=H*FACTOR
  L=L*FACTOR*(1.E+03)
  CALL MSCUPF(W,S,T,H,L,ER,CO,CE)
  CALL MSCUPE(W,S,T,H,L,ER,CE0,CEE)
  AE=CE*CEE
  AO=CO*CE0
  BE=CEE/CE
  BO=CE0/CO
  ZOE=1./((3.0E+08)*SQRT(AE))
  ZOO=1./((3.0E+08)*SQRT(AO))
  AA=ZOE*ZOO
  ZO=SQRT(AA)
  VE=3.0E+08*SQRT(BE)
  VO=3.0E+08*SQRT(BO)
  VAVG=(VE+VO)/2.
  RHO=ZOE/ZOO
  C=(RHO-1.)/(RHO+1.)
  CDB=-20.*ALOG10(C)
  PRINT 5
5 FORMAT(1H0,1X,5HC(DB),3X,8HZ0(0HMS),2X,9HZ00(0HMS),2X,
19HZ0E(0HMS),5X,9HVE(M/SEC),5X,9HVE(M/SEC),5X,
211HVAVG(M/SEC))
  PRINT 6,CDB,ZO,ZOO,ZOE,VO,VE,VAVG
6 FORMAT(1H ,F5.2,5X,F6.2,5X,F6.2,5X,F6.2,5X,E10.3,5X,E10.3,
15X,E10.3)
  CO=CO*1.E+12
  CE=CE*1.E+12
  CE0=CE0*1.E+12
  CEE=CEE*1.E+12

```

```

      PRINT 7,C0,CE,CEE,CEE
7  FORMAT(1H0,7HCE(PF),F8.3,5X,7HCE(PF),F8.3,5X,
18HCEE(PF),F8.3,5X,8HCEE(PF),F8.3)
2  CONTINUE
   STOP
   END

```

```

SUBROUTINE MSCUPF(W,S,T,H,L,ER,C0,CE)
  DIMENSION N(6),X(46,6),Y(46,6),ALPHA(46,6),BETA1(46,6),
1BETA2(46,6),GAMMA(46,6),CH(46,6),SCH(6),TSCD(46,6,4),A(181,181),
2A1(132,132)
  REAL L
  COMMON/HELP/A,A1
  EQUIVALENCE (A,A1)
  N0=6
  N(1)=43
  N(2)=43
  N(3)=46
  N(4)=13
  N(5)=13
  N(6)=23
  E0=1/(4,*3.14159*2.99776*2.99776E+09)
  FACTOR=(1.0E-05)*(1./0.393700)
  KKK=0
  DELW=W/20,
  E=ER*E0
  X(1,1)=-(S/2.)-W
  Y(1,1)=H
  X(1,2)=-X(1,1)
  Y(1,2)=H
  DO 26 I=1,20
    IP1=I+1
    X(IP1,1)=X(I,1)+DELW
    Y(IP1,1)=H
    X(IP1,2)=X(I,2)-DELW
26  Y(IP1,2)=H
    X(22,1)=X(21,1)
    Y(22,1)=0.25*FACTOR*H
    X(22,2)=X(21,2)
    Y(22,2)=Y(22,1)
    DO 27 I=22,41
      IP1=I+1
      X(IP1,1)=X(I,1)-DELW
      Y(IP1,1)=Y(I,1)
      X(IP1,2)=X(I,2)+DELW
27  Y(IP1,2)=Y(I,2)
    X(43,1)=X(1,1)
    Y(43,1)=Y(1,1)
    X(43,2)=X(1,2)
    Y(43,2)=Y(1,2)
    DELL=L/45,
    X(1,3)=-L/2,

```

```

Y(1,3)=0,
D0 28 I=1,45
IP1=I+1
X(IP1,3)=X(I,3)+DELL
28 Y(IP1,3)=0.
DELL=H/2,
X(1,4)=X(1,3)
Y(1,4)=0,
X(1,5)=L/2,
Y(1,5)=0,
D0 29 I=1,2
IP1=I+1
X(IP1,4)=X(1,4)
Y(IP1,4)=Y(I,4)+DELH
X(IP1,5)=X(1,5)
29 Y(IP1,5)=Y(I,5)+DELH
DEL=(L/2,*(S/2.+W))/10.
D0 30 I=3,12
IP1=I+1
X(IP1,4)=X(I,4)+DEL
Y(IP1,4)=H
X(IP1,5)=X(I,5)-DEL
30 Y(IP1,5)=H
X(1,6)=-S/2,-W
Y(1,6)=H*0.25*FACTOR
X(21,6)=S/2,+W
Y(21,6)=Y(1,6)+T
DELT=T/2,
D0 31 I=1,2
IP1=I+1
IP21=I+21
IP21M1=IP21-1
X(IP1,6)=X(I,6)
Y(IP1,6)=Y(I,6)+DELT
X(IP21,6)=X(IP21M1,6)
31 Y(IP21,6)=Y(IP21M1,6)-DELT
DELOV=(2*W+S)/18,
D0 32 I=3,20
IP1=I+1
X(IP1,6)=X(I,6)+DELOV
32 Y(IP1,6)=Y(I,6)
D0 47 LLL=1,2
IF(KKK=0) 38,37,38
C ODD MODE
37 CONTINUE
D0 332 J=1,2
D0 33 I=1,42
ALPHA(I,J)=1.
BETA1(I,J)=0.
BETA2(I,J)=0.
GO TO (34,35),J
34 GAMMA(I,J)=1.
GO TO 33

```

```

35 GAMMA(I,J)=-1.
33 CONTINUE
332 CONTINUE
   KKK=KKK+1
   GO TO 39
EVEN MODE
38 CONTINUE
   DO 40 J=1,2
   DO 41 I=1,42
     ALPHA(I,J)=1.
     BETA1(I,J)=0.
     BETA2(I,J)=0.
42 GAMMA(I,J)=1.
41 CONTINUE
40 CONTINUE
39 CONTINUE
   DO 36 I=1,45
     ALPHA(I,3)=1.
     BETA1(I,3)=0.
     BETA2(I,3)=0.
36 GAMMA(I,3)=0.
   DO 45 I=1,12
     ALPHA(I,4)=0.
     BETA1(I,4)=E
     BETA2(I,4)=E0
     GAMMA(I,4)=0.
     ALPHA(I,5)=0.
     BETA1(I,5)=E0
     BETA2(I,5)=E
45 GAMMA(I,5)=0.
   DO 46 I=1,22
     ALPHA(I,6)=0.
     BETA1(I,6)=E
     BETA2(I,6)=E0
46 GAMMA(I,6)=0.
   XMIN=0,
   XMAX=0,
   YMIN=0,
   YMAX=0,
   NX=0
   NY=0
   IDIM=46
   R=1.0E+05
   NAXDIM=181
   NAYDIM=181
   CALL LPLACF(N0,N,X,Y,ALPHA,BETA1,BETA2,GAMMA,CH,SCH,IDIM,R,TSCD,
1XMIN,XMAX,NX,YMIN,YMAX,NY,NAXDIM,NAYDIM)
   DELF=W/20,
   DELE=0.25*FACTOR
   FF1=6,2831852*E*DELF
   FF2=6,2831852*E*DELE
   FF4=6,2831852*E0*DELE

```

```

      CHRG=0,
      DO 50 I=1,20
50    CHRG=CHRG+FF1*CH(I,1)
      DO 51 I=22,41
51    CHRG=CHRG+FF1*CH(I,1)
      CHRG=CHRG+(FF2*CH(21,1)+FF4*CH(42,1))
      IF (LLL.EQ,2) GO TO 60
      CO=CHRG
      GO TO 47
60    CE=CHRG
47    CONTINUE
      RETURN
      END

```

```

SUBROUTINE LPLACF(N0,N,X,Y,ALPHA,BETA1,BETA2,GAMMA,CH,SCH,IDIM,R,
1  TSCD,XMIN,XMAX,NX,YMIN,YMAX,NY,NAXDIM,NAYDIM)
  DIMENSION X(IDIM,N0),Y(IDIM,N0),ALPHA(IDIM,N0),BETA1(IDIM,N0),
1BETA2(IDIM,N0),GAMMA(IDIM,N0),CH(IDIM,N0),TSCD(IDIM,N0,4),N(N0),
2A(181,181),SCH(N0),B(175),A1(132,132)
  COMMON/HELP/A,A1
  EQUIVALENCE (A,A1)
  PI=3.1415926
  RR=R*R
  DO 1 L=1,N0
  NN=N(L)-1
  DO 1 I=1,NN
  XI=X(I+1,L)-X(I,L)
  YI=Y(I+1,L)-Y(I,L)
  TSCD(I,L,1)=ATAN2(YI,XI)
  TSCD(I,L,2)=SIN(TSCD(I,L,1))
  TSCD(I,L,3)=COS(TSCD(I,L,1))
1  TSCD(I,L,4)=SQRT(XI*XI+YI*YI)
  JJJ=0
  DO 4 LJ=1,N0
  NJ=N(LJ)-1
  JAJ=JJJ
  JJJ=JJJ+NJ
  DO 4 J=1,NJ
  JJ=JAJ+J
  XJ=(X(J,LJ)+X(J+1,LJ))/2.
  YJ=(Y(J,LJ)+Y(J+1,LJ))/2.
  III=0
  DO 4 LI=1,N0
  NI=N(LI)-1
  III=III+NI
  IAI=III-NI
  DO 4 I=1,NI
  II=IAI+I
  IF(II,EQ,JJ) GO TO 3
  X1=XJ-X(I,LI)
  X2=XJ-X(I+1,LI)
  Y1=YJ-Y(I,LI)

```

```

Y2=YJ-Y(I+1,L1)
R1=X1*X1+Y1*Y1
R2=X2*X2+Y2*Y2
S1=0,
S2=0,
YT=Y(I,L1)*X2-Y(I+1,L1)*X1+YJ*(X(I+1,L1)-X(I,L1))
XT=X1*X2+Y1*Y2
TETA=ATAN2(YT,XT)
IF (ALPHA(J,LJ).EQ.0,) GO TO 2
S1=TSCD(I,L1,4)*(1.=0.5*ALOG(R2/RR))+0.5*ALOG(R2/R1)*(X1*TSCD(I,L1
1,3)+Y1*TSCD(I,L1,2))+TETA*(X1*TSCD(I,L1,2)-Y1*TSCD(I,L1,3))
2 TETA1=TSCD(J,LJ,1)-TSCD(I,L1,1)
S2=0.5*SIN(TETA1)*ALOG(R2/R1)+COS(TETA1)*TETA
S3=-S2
GO TO 4
3 S1=TSCD(I,L1,4)*(1.=ALOG(TSCD(I,L1,4)/2./R))
S2=-PI
S3=-PI
4 A(JJ,I)=ALPHA(J,LJ)*S1+BETA1(J,LJ)*S2+BETA2(J,LJ)*S3
M=0
DO 5 L=1,N0
5 M=M+N(L)-1
JJJ=0
DO 6 L=1,N0
NN=N(L)-1
JAJ=JJJ
JJJ=JJJ+NN
DO 6 J=1,NN
JJ=JAJ+J
6 B(JJ)=GAMMA(J,L)
CALL ARRAY(2,M,M,NAXDIM,NAYDIM,A,A)
CALL SIMQ(A,B,M,KS)
IF (KS.NE.0) PRINT 100
100 FORMAT(1H0,10HSYSTEM IS SINGULAR)
JJJ=0
DO 7 L=1,N0
NN=N(L)-1
JAJ=JJJ
JJJ=JJJ+NN
DO 7 J=1,NN
JJ=JAJ+J
7 CH(J,L)=B(JJ)
DO 8 L=1,N0
NN=N(L)-1
SCH(L)=0,
DO 8 I=1,NN
8 SCH(L)=SCH(L)+TSCD(I,L,4)*CH(I,L)
IF (NX=1) 17,9,10
9 DX=0,
GO TO 11
10 DX=(XMAX-XMIN)/FLOAT(NX=1)
11 IF (NY=1) 17,12,13

```

```

12 DY=0,
   GO TO 14
13 DY=(YMAX-YMIN)/FLOAT(NY=1)
14 DO 16 II=1,NX
   XJ=XMIN+FLOAT(II-1)*DX
   DO 16 JJ=1,NY
   YJ=YMIN+FLOAT(JJ-1)*DY
   A(II,JJ)=0.
   DO 16 LI=1,N0
   NN=N(LI)=1
   DO 16 I=1,NN
   X1=XJ=X(I,LI)
   X2=XJ=X(I+1,LI)
   Y1=YJ=Y(I,LI)
   Y2=YJ=Y(I+1,LI)
   R1=X1*X1+Y1*Y1
   R2=X2*X2+Y2*Y2
   IF((R1.EQ.0.).OR.(R2.EQ.0.)) GO TO 15
   YT=Y(I,LI)*X2-Y(I+1,LI)*X1+YJ*(X(I+1,LI)-X(I,LI))
   XT=X1*X2+Y1*Y2
   TETATAN2(YT,XT)
   S1=TSKD(I,LI,4)*(1.=0.5*ALOG(R2/RR))+0.5*ALOG(R2/R1)*(X1*TSKD(I,LI
1,3)+Y1*TSKD(I,LI,2))+TETA*(X1*TSKD(I,LI,2)-Y1*TSKD(I,LI,3))
   GO TO 16
15 S1=TSKD(I,LI,4)*(1.=0.5*ALOG((R1+R2)/RR))
16 A(II,JJ)=A(II,JJ)+S1*CH(I,LI)
17 RETURN
   END

```

```

SUBROUTINE MSCUPE(W,S,T,H,L,RR,C0,C5)
  DIMENSION N(3),X(46,3),Y(46,3),ALPHA(46,3),BETA1(46,3),
1BETA2(46,3),GAMMA(46,3),CH(46,3),SCH(3),TSKD(46,3,4),A(181,181),
2A1(132,132)
  COMMON/HELP/A,A1
  EQUIVALENCE (A,A1)
  REAL L
  E0=1./((4.*3.14159*2.99776*2.99776E+09)
  FACTOR=(1.0E-05)*(1./0.393700)
  N0=3
  N(1)=43
  N(2)=43
  N(3)=46
  KKK=0
  DELW=W/20,
  E=ER=E0
  X(1,1)=-(S/2.)*W
  Y(1,1)=H
  X(1,2)=-X(1,1)
  Y(1,2)=H
  DO 26 I=1,20
  IP1=I+1
  X(IP1,1)=X(I,1)+DELW

```

```

      Y(IP1,1)=H
      X(IP1,2)=X(I,2)*DELW
26  Y(IP1,2)=H
      X(22,1)=X(21,1)
      Y(22,1)=0.25*FACTOR*H
      X(22,2)=X(21,2)
      Y(22,2)=Y(22,1)
      DO 27 I=22,41
        IP1=I+1
        X(IP1,1)=X(I,1)*DELW
        Y(IP1,1)=Y(I,1)
        X(IP1,2)=X(I,2)*DELW
27  Y(IP1,2)=Y(I,2)
      X(43,1)=X(1,1)
      Y(43,1)=Y(1,1)
      X(43,2)=X(1,2)
      Y(43,2)=Y(1,2)
      DELL=L/45,
      X(1,3)=-L/2,
      Y(1,3)=0,
      DO 28 I=1,45
        IP1=I+1
        X(IP1,3)=X(I,3)+DELL
28  Y(IP1,3)=0,
      DO 47 LLL=1,2
        IF(KKK=0) 38,37,38
C   ODD MODE
37  CONTINUE
      DO 332 J=1,2
      DO 33 I=1,42
        ALPHA(I,J)=1.
        BETA1(I,J)=0.
        BETA2(I,J)=0.
        GO TO (34,35),J
34  GAMMA(I,J)=1.
      GO TO 33
35  GAMMA(I,J)=-1.
33  CONTINUE
:332 CONTINUE
      KKK=KKK+1
      GO TO 39
C   EVEN MODE
38  CONTINUE
      DO 40 J=1,2
      DO 41 I=1,42
        ALPHA(I,J)=1.
        BETA1(I,J)=0.
        BETA2(I,J)=0.
42  GAMMA(I,J)=1.
41  CONTINUE
40  CONTINUE
39  CONTINUE

```

```

DO 36 I=1,45
ALPHA(I,3)=1.
BETA1(I,3)=0.
BETA2(I,3)=0.
36 GAMMA(I,3)=0.
XMIN=0.
XMAX=0.
YMIN=0.
YMAX=0.
NX=0
NY=0
IDIM=46
R=1.0E+05
NAXDIM=132
NAYDIM=132
CALL LPLACE(N0,N,X,Y,ALPHA,BETA1,BETA2,GAMMA,CH,SCH,IDIM,R,TSCD,
1XMIN,XMAX,NX,YMIN,YMAX,NY,NAXDIM,NAYDIM)
IF (LLL.EQ.2) GO TO 50
CEE=2,*3,14159*0.855E-12*SCH(1)
GO TO 47
50 CEE=2,*3,14159*0.855E-12*SCH(1)
47 CONTINUE
RETURN
END

```

```

SUBROUTINE LPLACE(N0,N,X,Y,ALPHA,BETA1,BETA2,GAMMA,CH,SCH,IDIM,R,
1TSCD,XMIN,XMAX,NX,YMIN,YMAX,NY,NAXDIM,NAYDIM)
DIMENSION X(IDIM,N0),Y(IDIM,N0),ALPHA(IDIM,N0),BETA1(IDIM,N0),
1BETA2(IDIM,N0),GAMMA(IDIM,N0),CH(IDIM,N0),TSCD(IDIM,N0,4),N(N0),
2A1(132,132),SCH(N0),B(129),A(181,181)
COMMON/HELP/A,A1
EQUIVALENCE (A,A1)
PI=3,1415926
RR=R*R
DO 1 L=1,N0
NN=N(L)-1
DO 1 I=1,NN
XI=X(I+1,L)-X(I,L)
YI=Y(I+1,L)-Y(I,L)
TSCD(I,L,1)=ATAN2(YI,XI)
TSCD(I,L,2)=SIN(TSCD(I,L,1))
TSCD(I,L,3)=COS(TSCD(I,L,1))
1 TSCD(I,L,4)=SQRT(XI*XI+YI*YI)
JJJ=0
DO 4 LJ=1,NJ
NJ=N(LJ)-1
JAJ=JJJ
JJJ=JJJ+NJ
DO 4 J=1,NJ
JJ=JAJ+J
XJ=(X(J,LJ)+X(J+1,LJ))/2.
YJ=(Y(J,LJ)+Y(J+1,LJ))/2.

```

```

      III=0
      DO 4 LI=1,N0
      NI=N(LI)-1
      III=III+NI
      IAI=III-NI
      DO 4 I=1,NI
      II=IAI+I
      IF(II,EQ,JJ) GO TO 3
      X1=XJ=X(I,LI)
      X2=XJ=X(I+1,LI)
      Y1=YJ=Y(I,LI)
      Y2=YJ=Y(I+1,LI)
      R1=X1*X1+Y1*Y1
      R2=X2*X2+Y2*Y2
      S1=0,
      S2=0,
      YT=Y(I,LI)*X2-Y(I+1,LI)*X1+YJ*(X(I+1,LI)-X(I,LI))
      XT=X1*X2+Y1*Y2
      TETA=ATAN2(YT,XT)
      IF(ALPHA(J,LJ),EQ,0,) GO TO 2
      S1=TSCD(I,LI,4)*(1.=0.5*ALOG(R2/RR))+0.5*ALOG(R2/R1)*(X1*TSCD(I,LI
1,3)+Y1*TSCD(I,LI,2))+TETA*(X1*TSCD(I,LI,2)-Y1*TSCD(I,LI,3))
2  TETA1=TSCD(J,LJ,1)-TSCD(I,LI,1)
      S2=0.5*SIN(TETA1)*ALOG(R2/R1)+COS(TETA1)*TETA
      S3=-S2
      GO TO 4
3  S1=TSCD(I,LI,4)*(1.=ALOG(TSCD(I,LI,4)/2,/R))
      S2=-PI
      S3=-PI
4  A1(JJ,II)=ALPHA(J,LJ)*S1+BETA1(J,LJ)*S2+BETA2(J,LJ)*S3
      M=0
      DO 5 L=1,N0
5  M=M+N(L)-1
      JJJ=0
      DO 6 L=1,N0
      NN=N(L)-1
      JAJ=JJJ
      JJJ=JJJ+NN
      DO 6 J=1,NN
      JJ=JAJ+J
6  B(JJ)=GAMMA(J,L)
      CALL ARRAY(2,M,M,NAXDIM,NAYDIM,A1,A1)
      CALL SIMQ(A1,B,M,KS)
      IF (KS,NE,0) PRINT 100
100 FORMAT(1H0,10HSYSTEM IS SINGULAR)
      JJJ=0
      DO 7 L=1,N0
      NN=N(L)-1
      JAJ=JJJ
      JJJ=JJJ+NN
      DO 7 J=1,NN
      JJ=JAJ+J
7  CH(J,L)=B(JJ)

```

```

      DO 8 L=1,N0
      NN=N(L)-1
      SCH(L)=0,
      DO 8 I=1,NN
8     SCH(L)=SCH(L)+TSCD(I,L,4)*CH(I,L)
      IF(NX=1)17,9,10
9     DX=0,
      GO TO 11
10    DX=(XMAX-XMIN)/FLOAT(NX=1)
11    IF(NY=1)17,12,13
12    DY=0,
      GO TO 14
13    DY=(YMAX-YMIN)/FLOAT(NY=1)
14    DO 16 II=1,NX
      XJ=XMIN+FLOAT(II-1)*DX
      DO 16 JJ=1,NY
      YJ=YMIN+FLOAT(JJ-1)*DY
      A1(II,JJ)=0,
      DO 16 LI=1,N0
      NN=N(LI)-1
      DO 16 I=1,NN
      X1=XJ-X(I,LI)
      X2=XJ-X(I+1,LI)
      Y1=YJ-Y(I,LI)
      Y2=YJ-Y(I+1,LI)
      R1=X1*X1+Y1*Y1
      R2=X2*X2+Y2*Y2
      IF((R1.EQ,0,).OR.(R2.EQ,0,)) GO TO 15
      YT=Y(I,LI)*X2-Y(I+1,LI)*X1+YJ*(X(I+1,LI)-X(I,LI))
      XT=X1*X2+Y1*Y2
      TETA=ATAN2(YT,XT)
      S1=TSCD(I,LI,4)*(1.=0,5*ALOG(R2/RR))+0,5*ALOG(R2/R1)*(X1*TSCD(I,LI
1,3)+Y1*TSCD(I,LI,2))+TETA*(X1*TSCD(I,LI,2)-Y1*TSCD(I,LI,3))
      GO TO 16
15    S1=TSCD(I,LI,4)*(1.=0,5*ALOG((R1+R2)/RR))
16    A1(II,JJ)=A1(II,JJ)+S1*CH(I,LI)
17    RETURN
      END

```

```

      SUBROUTINE ARRAY (MODE,I,J,N,M,S,D)
      DIMENSION S(1),D(1)
      NI=N-I
      IF(MODE=1) 100,100,120
100   IJ=I*J+1
      NM=N*J+1
      DO 110 K=1,J
      NM=NM-NI
      DO 110 L=1,I
      IJ=IJ+1
      NM=NM-1
110   D(NM)=S(IJ)
      GO TO 140
120   IJ=0

```

```

NM=0
DO 130 K=1,J
DO 125 L=1,I
IJ=IJ+1
NM=NM+1
125 S(IJ)=D(NM)
130 NM=NM+NI
140 RETURN
END

```

```

SUBROUTINE SIMQ(A,B,N,KS)
DIMENSION A(1),B(1)
TOL=0.0
KS=0
JJ=-N
DO 65 J=1,N
JY=J+1
JJ=JJ+N+1
BIGA=0.
IT=JJ=J
DO 30 I=J,N
IJ=IT+I
IF(ABS(BIGA)-ABS(A(IJ))) 20,30,30
20 BIGA=A(IJ)
IMAX=I
30 CONTINUE
IF(ABS(BIGA)-TOL) 35,35,40
35 KS=1
RETURN
40 I1=J+N*(J=2)
IT=IMAX-J
DO 50 K=J,N
I1=I1+N
I2=I1+IT
SAVE=A(I1)
A(I1)=A(I2)
A(I2)=SAVE
50 A(I1)=A(I1)/BIGA
SAVE=B(IMAX)
B(IMAX)=B(J)
B(J)=SAVE/BIGA
IF(J=N) 55,70,55
55 IQS=N*(J=1)
DO 65 IX=JY,N
IXJ=IQS+IX
IT=J=IX
DO 60 JX=JY,N
IXJX=N*(JX-1)+IX
JXJX=IXJX+IT
60 A(IXJX)=A(IXJX)-(A(IXJ)*A(JXJX))
65 B(IX)=B(IX)-(B(J)*A(IXJ))
70 NY=N-1

```

## NRL REPORT 7810

```
IT=N*N
DO 80 J=1,NY
IA=IT-J
IB=N-J
IC=N
DO 80 K=1,J
B(IB)=B(IB)-A(IA)*B(IC)
IA=IA-N
80 IC=IC-1
RETURN
END
```

